Materials and Design 155 (2018) 86–98

Contents lists available at ScienceDirect

Materials and Design

journal homepage: www.elsevier.com/locate/matdes

Fabrication of polymeric lattice structures for optimum energy absorption using Multi Jet Fusion technology

F.N. Habib *, P. Iovenitti, S.H. Masood, M. Nikzad

Department of Mechanical and Product Design Engineering, Faculty of Science, Engineering and Technology, Swinburne University of Technology, Melbourne 3122, Australia

HIGHLIGHTS

- Designing polymeric periodic lattice structures of identical relative density from six different unit cells
- Successful fabrication of the lattices via Multi Jet Fusion (MJF)
- Characterization of their quasi-static energy absorption behaviour using FEA and experimental validation
- The lattice of octagonal unit cell provides the optimum energy absorption characteristics.
- MJF can produce polymeric lattices of much better quality with dramatically reduced time than traditional FDM.

GRAPHICAL ABSTRACT

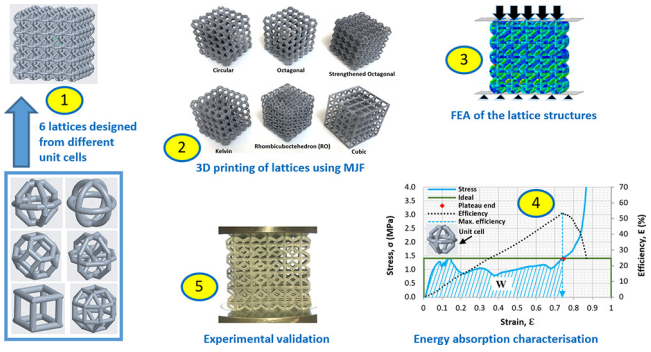

ARTICLE INFO

Article history:
Received 24 April 2018
Received in revised form 25 May 2018
Accepted 27 May 2018
Available online 29 May 2018

Keywords:
Lattice structure
Cell topology
3D printing
Multi Jet Fusion
Finite element analysis
Energy absorption

ABSTRACT

Unlike stochastic foams, 3D printed lattice structures can be created with a tailored microstructure to achieve the desired global mechanical properties. In this study, quasi-static energy absorption of six polymeric lattice structures of different unit cell topologies and deformation behaviours but with identical relative density are investigated. For the first time, a recently developed powerful 3D printing technology, namely Multi Jet Fusion (MJF), is utilized to produce high quality and performance lattices. Nonlinear finite element analysis (FEA) is used to analyse their compressive response and energy-absorbing characteristics. To validate the FEA results, experimental compression tests are performed on two types of lattices. The results of this investigation showed that the global energy absorption of lattices can be improved through controlling and manipulating their micro-topology. It is found that the lattice structures with bending-dominated deformation have low stiffness and strength but provide good energy absorption capability. The stretch and buckling dominated structures are shown to be stiffer and stronger but have low energy absorption performance. The findings of this research identify high performing unit cell geometries that can be used for energy absorption application of lattice structures in the development of advanced 3D printed structures that are superior to stochastic foams.

1. Introduction

One of the major uses of cellular materials is in energy absorption applications, such as packaging and protective devices. They can undergo a large compressive strain at nearly a constant stress level, thus absorbing a large amount of energy without producing a high stress on the protected object. This makes them excellent for such applications because the aim of using energy-absorbing materials is not just to absorb a certain amount of energy, but also to keep the transmitted force to the protected object below the threshold that can cause damage or injury [1]. Foams are the most well-known type of cellular materials

* Corresponding author.
E-mail address: fhabib@swin.edu.au (F.N. Habib).

https://doi.org/10.1016/j.matdes.2018.05.059
0264-1275/

Table 1
Unit cell and overall specimen design and dimensions for the examined 3D structures of 15% relative density.

Structure type	Lattice designation	Unit cell design	Cell design parameters		A 2 × 2 × 2 cells structure showing the way the cells joined together	Overall cubic spacemen	
			D or *l* (mm)	*d* (mm)		CAD model	Side length (mm)
1	Circular	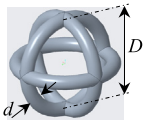	$D = 10$	1.488	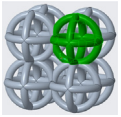	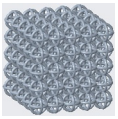	51.488
2	Octagonal	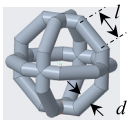	$l = 4.14$	1.626	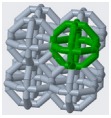	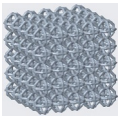	51.626
3	Strengthened Octagonal	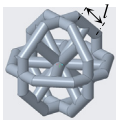	$l = 4.14$	*1.214*	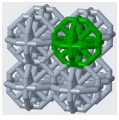	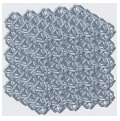	51.214
4	Kelvin	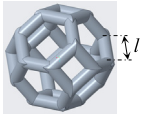	$l = 3.54$	1.496	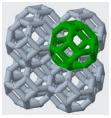	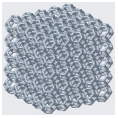	51.496
5	Rhombicuboctahedron (RO)	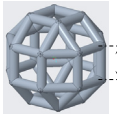	$l = 4.14$	1.134	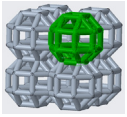	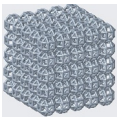	51.134
6	Cubic	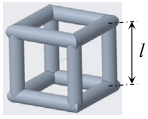	$l = 10$	2.246	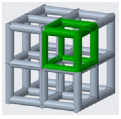	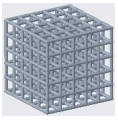	52.246

that are widely used. Polymeric and metallic foams are tailored for a specific energy absorption application by choosing the right material and density. However, the drawback of foams is they are stochastic and have a random microstructure [2]. As the structure of these materials at the micro level play a big role in their global behaviour and properties [3,4], researchers have tried to find better alternatives for foams. Lattice materials (structures) fabricated by 3D printing can overcome this limitation to a great extent. By exploiting this advantage offered by 3D printing technology, lattice materials can be made with uniform and ordered microstructure, their unit cells can be manipulated and optimized to attain the desired mechanical properties for a particular application [2].

Lattice structures are commonly constructed by duplicating three-dimensional mesoscale unit cells. They are multi-functional materials that can offer a range of desirable properties. They offer the potential to easily engineer specific meso-scale properties (at cell level) to produce desirable macro-scale material properties for a wide variety of engineering applications [5].

Several researchers have investigated the influence of unit cell shape on compressive strength of lattice structures especially for bio-based tissue engineering (TE) scaffolds [6–10]. Others have studied the effect of the unit cell on the global deformation and crushing behaviour of cellular structures. For instance, Li et al. [11] showed that the unit cell shape design is an effective way to control the mechanical properties of the reticulate meshes such as the elastic modulus, compressive strength and deformation behaviour. Ashby [3] considered the distinction between stretch-dominated and bending-dominated structures the most important concept in analysing the mechanical behaviour of lattice materials. For a given density, the first is extremely stiff and strong, while the second is compliant and not strong, but absorbs energy well during compression. Ahmadi et al. [12] experimentally showed that the mechanical properties, compressive behaviour and failure mechanism of 3D printed porous titanium alloy biomaterials were highly dependent upon the type and dimensions of the building unit cells. Craddock et al. [13] indicated that despite the current limitation of additive manufacturing techniques they can be used for manufacturing tailored lattice structures for impact absorption. Vesenjak et al. [14] experimentally studied the influence of cell shape on the compressive behaviour and energy absorption of 2D polymeric cellular structures with quadratic and circular cells under quasi-static and dynamic uniaxial compressive loading. Hammetter et al. [15] investigated the effect of strut slenderness, strut inclination angle, and number of repeat lattice layers on the mechanics of compressive deformation including the specific strength and energy absorption of pyramidal lattice structures using analytical and numerical methods. Ozdemir et al. [5,16] experimentally and numerically studied the energy absorption of additively manufactured metallic lattice structures of cubic, diamond and re-intrant lattice structures under quasi-static and dynamic loading. Ullah et al. [17] used single unit cell approach to predict the energy absorption capacity of Kagome and atomic truss configurations built through selective laser melting via experimental and numerical studies. Gautam et al. [18] studied the influence of build orientation, truss radius and surface roughness on stiffness, strength and energy absorption of ABS Kagome truss single unit cells built via fused deposition modeling (FDM). Ha et al. [19] designed and studied an energy absorbing lattice constructed from multiple tetra-beam-plate unit cells with negative stiffness behaviour. The lattice was fabricated by selective laser sintering (SLS) approach and analysed both numerically and experimentally. Kaur et al. [20] investigated the deformation of two types of 3D printed stretch-dominated micro-lattice structures made of different polymeric materials using compression testing and FEA simulation methods. Choy et al. [21] investigated the mechanical

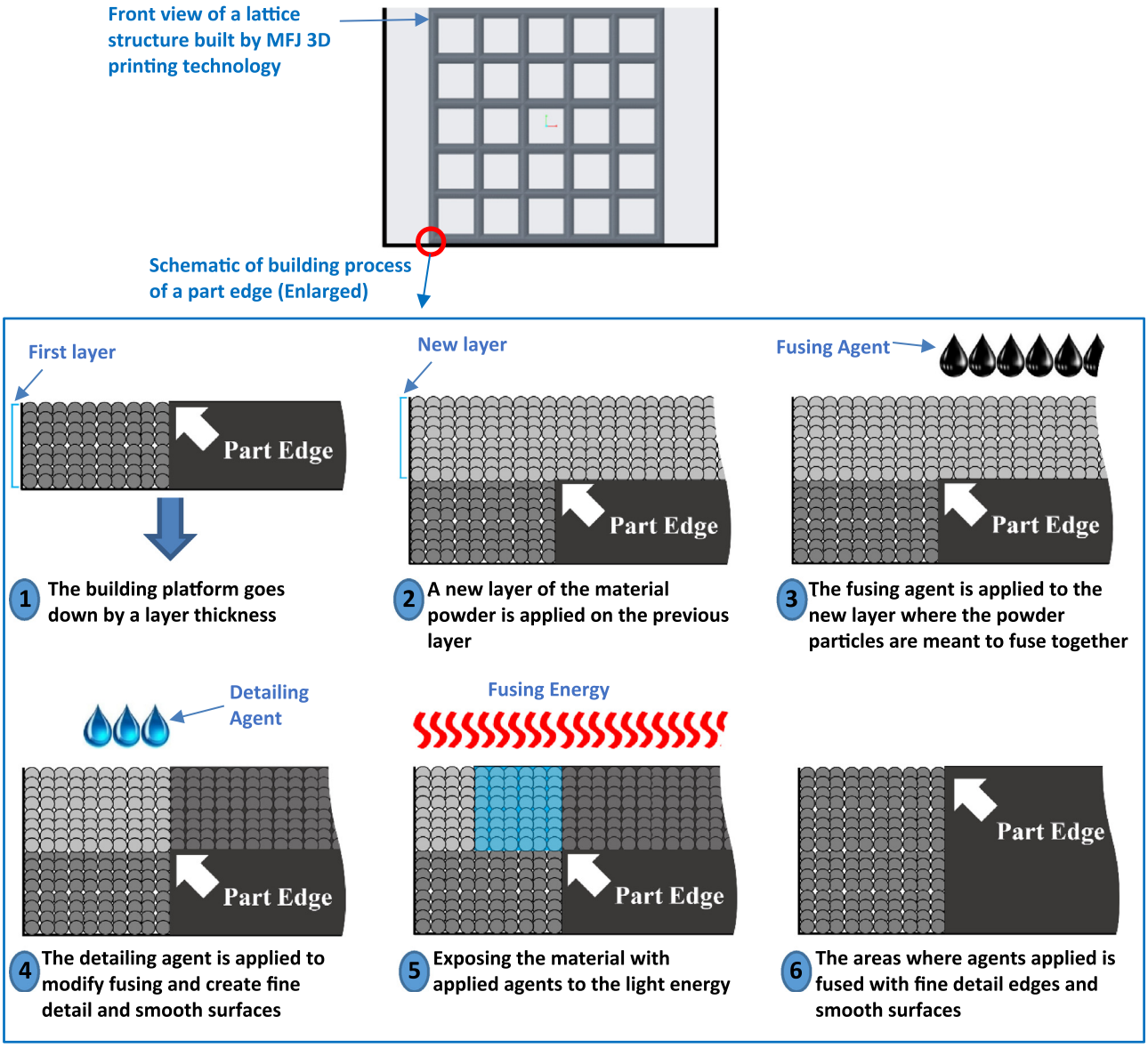

Fig. 1. Schematic of building process in Multi Jet Fusion (MJF) system.

properties of density graded metallic lattice structures of cubic and hexagonal unit cells fabricated by selective laser melting (SLM). Al-Saedi et al. [22] studied the compressive properties and energy absorption capability of functionally graded aluminum alloy lattice fabricated by SLM. Harris et al. [23] experimentally investigated the impact response of additively manufactured stainless steel hybrid lattice materials. Winter et al. [24] numerically studied the dynamic energy absorption behaviour of a series of two-dimensional stainless steel cellular structures of different architectures. Mohsenizadeh et al. [25] experimentally showed that it is possible to design and additively manufacture lightweight polymeric metamaterials for energy absorption capable of recovering their shape after high deformation.

While most of the published works have investigated the behaviour of specific types of individual lattice structures with specific unit cell geometry, very few studies have been made to compare the mechanical response and energy absorption characteristic of 3D printed lattices of different types of unit cells made of identical relative density. Researchers have also been able to design and 3D print energy absorbing lattice structures, but still more detailed studies are required to identify the idealised geometry of the unit cell, which will generate a lattice capable of absorbing maximum energy at the lowest transmitted stress level.

This work examines the effect of a variety of 3D unit cell topologies on the energy absorption behaviour and compressive response of the respective 3D printed polymeric lattice structures of uniform relative density. The aim is the development of a high energy-absorbing lattice with the closest behaviour to the ideal energy absorber (the highest specific energy absorption at lowest stress level). Full-scale nonlinear finite element analysis (FEA) method was used to simulate their compressive behaviour under uniaxial quasi-static loading. Experimental compressive tests are performed to validate the FEA results with lattice structures printed on a newly developed powerful 3D system, namely Multi Jet Fusion (MJF), in a new brand of polyamide 12 material namely HP PA12A available on the system. A systematic approach is presented to characterise and investigate the energy absorption properties of the 3D lattice structures and a clear criterion is set to identify the best structures. The global stress-strain behaviour and the energy absorption performance of the structures are related to the deformation behaviour of their building unit cells. The optimum lattice for energy absorption applications is identified.

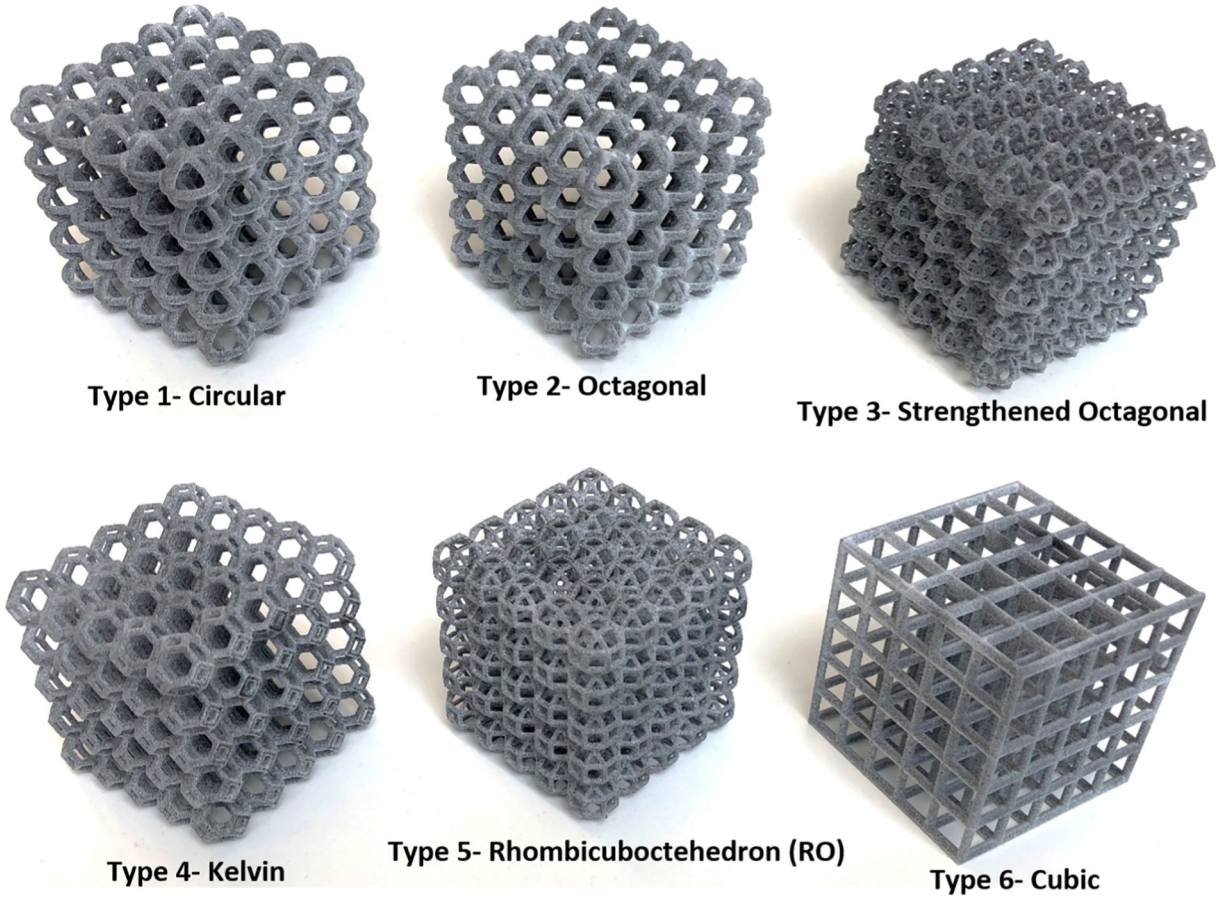

Fig. 2. 3D printed prototypes of the lattice structures on HP Jet Fusion 4200 3D printing machine in polyamide 12 (HP PA12).

2. Design and material

2.1. Lattices design

The relative density is the single most important feature of cellular solids [1]. It is the ratio of the apparent density of a cellular material, ρ^*, to that of the parent solid material from which the cell edges are made, ρ_s. It is also equal to the volume fraction of solid in the cellular material. In this study, to investigate the compressive response and energy absorption performance of ordered lattice structures, this parameter was kept constant.

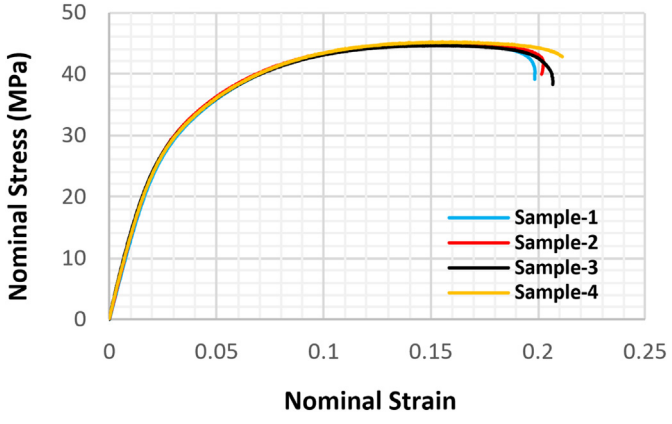

Fig. 3. Stress-strain curves obtained from standard tensile testing of HP PA12 coupons (specimen Type I, ASTM D638-14).

Six types of cellular structures were designed from different unit cells. The unit cell shapes were chosen in a way that provides different deformation mechanisms of the cell edges, such as bending, stretching and buckling. Each unit cell had centre line dimensions of 10 × 10 × 10 mm^3 and was geometrically symmetric around the three perpendicular planes intersected at its central point. Each lattice structure consisted of 5 × 5 × 5 cells constructed by duplicating unit cells in the three directions. The six structures were designed to have a constant relative density of 15%. Table 1 shows the computer-aided design (CAD) models of the six building unit cells, the way they were joined together, the 3D lattice specimens constructed from each unit cell, and their dimensions. It can be observed from Table 1 that the unit cells that have more edge members have their struts' diameter thinner in order to keep the relative density constant.

The unit cell of type 1 (Table 1) is a bending dominated structure, built from three perpendicular crossed rings (designated as Circular lattice). In a previous study [26] on the cell geometry effect on in-plane energy absorption behaviour of 2D honeycomb structures, it was shown that the octagonal honeycomb could provide the optimum energy absorption performance after the hexagonal honeycomb. As hexagonal cell geometry was not easy to pack in three dimensions, and so an octagonal cell was chosen for constructing 3D lattice in this work. Thus type 2 was constructed from three crossed octagons, designated as Octagonal lattice. Its deformation mechanism under uniaxial compressive loading is a combination of bending and buckling of the cell edges. These two types of lattices (type 1 and 2) have been also investigated for tissue engineering scaffolds [6]. Some internal struts were added to strengthen the Octagonal lattice and form type 3 which was designated as Strengthen Octagonal lattice. It was shown that the vertical edges in the loading direction, which deform by buckling during the loading, cause instability and undulating behaviour of stress in the plateau

Table 2
Material properties of HP PA12 determined from the standard tensile test (ASTM D638-14).

(a) Physical and elastic properties								
Material	Elastic modulus		Poisson's ratio[a]		Density[b]		0.2% offset yield strength	
HP PA12	1340 (MPa)		0.33		919 kg/m^3		22.8 (MPa)	
(b) Post-yield true stress versus true plastic strain								
Yield stress (MPa)	22.8	27.6	31.3	35.6	40.9	47.6	51.0	51.7
Plastic strain	0.000	0.007	0.014	0.025	0.045	0.085	0.129	0.150

[a] From FDM Nylon12 [37].
[b] Measured.

region, which is not preferred for energy absorbing applications [26]. That's why the added struts in type 3 were inclined and not vertical. Lattice type 4 was built from tetrakaidekahedron cells, known as Kelvin cells, which is used for representing, idealizing and modeling of stochastic foams [27–29] due to its bending dominated deformation. Type 5 is constructed from rhombicuboctahedron (RO) cells and it has been investigated for TE scaffold application [6,30,31]. Its deformation mechanism is stretching-dominated. Type 6 is constructed from simple cube cells which deform by buckling of the vertical struts under uniaxial compressive loading.

All unit cell struts have a circular cross-section of diameter "*d*". For unit cell of the Circular lattice type 1, "*D*" represents the diameter of the three crossed rings (refer to Table 1) and for all other unit cell types "*l*" represents the length of the equilateral members of polygons.

Choosing this wide range of different unit cells allows the energy absorption behaviour of lattices of different deformation mechanisms to be compared with each other.

2.2. Fabrication of lattices using Multi Jet Fusion process

In order to investigate the printability of the studied structures, a prototype of each lattice type was built using a new 3D printing technology called Multi Jet Fusion (MJF) in a brand of polyamide 12 plastic, namely HP PA12 available for this process. This recently developed technique can build plastic parts with high quality, functionality and dimensional accuracy much faster than the currently available 3D printing technologies [32]. Another important advantage of this new process is the parts made by this technique are almost isotropic, and their mechanical properties do not depend much on the building orientation.

A schematic of the building process in MJF system is shown in Fig. 1. In this technique, the building process begins by applying a thin layer of powder material on the building platform. Then, and in one continuous pass, the fusing agent is applied to the material layer where the powder particles are meant to fuse together, and the detailing agent is applied to modify fusing and create fine detail and smooth surfaces. This pass also combines the printing with fusing energy, and reactions between agents and the material cause the material to selectively fuse together to form the part.

Fig. 2 shows the printed prototypes of the investigated lattice structures built by HP Jet Fusion 4200 3D printing machine in HP PA12 material. It was observed that the dimensions, appearance, quality and details of the parts were very good.

3. Numerical simulation

3.1. Material characterization

To characterise the material properties of HP PA12, alongside with the lattices, four tensile standard test specimens of Type I with dimensions described in the standard test method for tensile properties of plastics, ASTM D638-14 [33], were built on HP Jet Fusion 4200 machine. The MTS Criterion Electromechanical Universal Test System (Model 43) with 50 kN load cell and an optical extensometer was used for the tensile test procedure at room temperature in accordance with ASTM D638-14. The resulting nominal stress-strain curves of the four samples under uniaxial tensile loading rate of 5 mm/min are shown in Fig. 3. The material behaviour of HP PA12 can be described as elastic, power hardening model [34]. It has relatively low yield stress but increases remarkably in the plastic region. The Abaqus plasticity with isotropic hardening model was used to define the material's behaviour. The elastic properties determined from the tensile tests are listed in Table 2a. The plastic nominal stress-strain data up to the necking obtained from the tensile

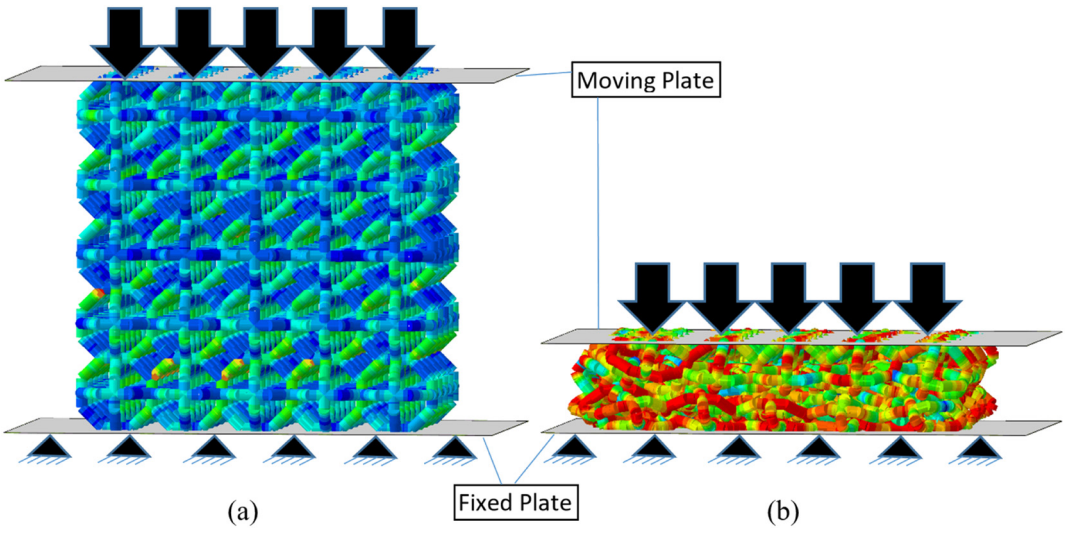

Fig. 4. (a) FEA setup and boundary conditions of a lattice structure (b) compressing the lattice by moving the top rigid plate with a constant speed towards the fixed bottom rigid plate.

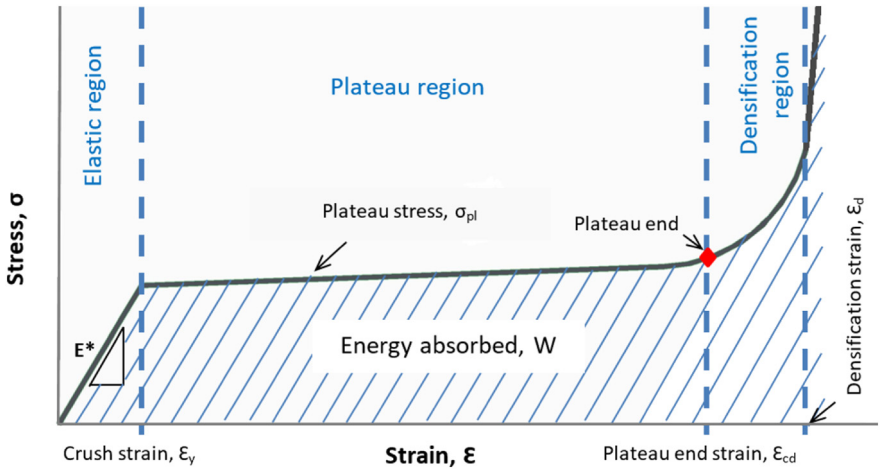

Fig. 5. Schematic compressive stress-strain behaviour of a cellular solid showing the three main regimes and the important parameters (reproduced from [37]).

tests was converted to true stress-strain data using the Eqs. (1) and (2) given in [35] and is listed in Table 2b. These values are used in the FEA to define the elastic and post-yield behaviour of HP PA12 as required by the Abaqus material model [36].

$$\sigma_{true} = \sigma_{\text{nominal}}(1 + \varepsilon_{\text{nominal}}) \quad (1)$$

$$\varepsilon_{true} = \ln(1 + \varepsilon_{\text{nominal}}) \quad (2)$$

3.2. Finite element analysis of the lattice structures

As the crushing mechanism of the lattices is a very complex process and involves all three types of nonlinearities, it cannot be simulated with implicit solvers. The three types of nonlinearities involved in the crushing of these structures include, firstly, the material nonlinearity, as the local stress in the cell struts exceeds the linear elastic limit of the parent material and it undergoes plastic deformation (yields), secondly, the geometrical nonlinearities due the large deformation of the structures, and the third type is the contact nonlinearity due to the interaction of struts during the crushing.

Abaqus/Explicit package [38] was employed to simulate the lattices' compressive behaviour under quasi-static uniaxial loading. The material properties determined from the tensile test and described in Section 3.1 were used as the material parameters input. Beam elements are the natural choice for discretisation of such lattice structures. They are computationally inexpensive and can be used to simulate models with many cells in a reasonable time [39]. Hence, the beam elements of type B31 [38], a 2-node linear beam in space, were used to model the lattices. Through convergence studies, it was found that the element global size smaller than 1.125 mm could not improve the accuracy of results much while significantly increasing the computational time. Thus, all the lattice structures were discretised with the element size of 1.125 mm. The compression simulation was performed using two

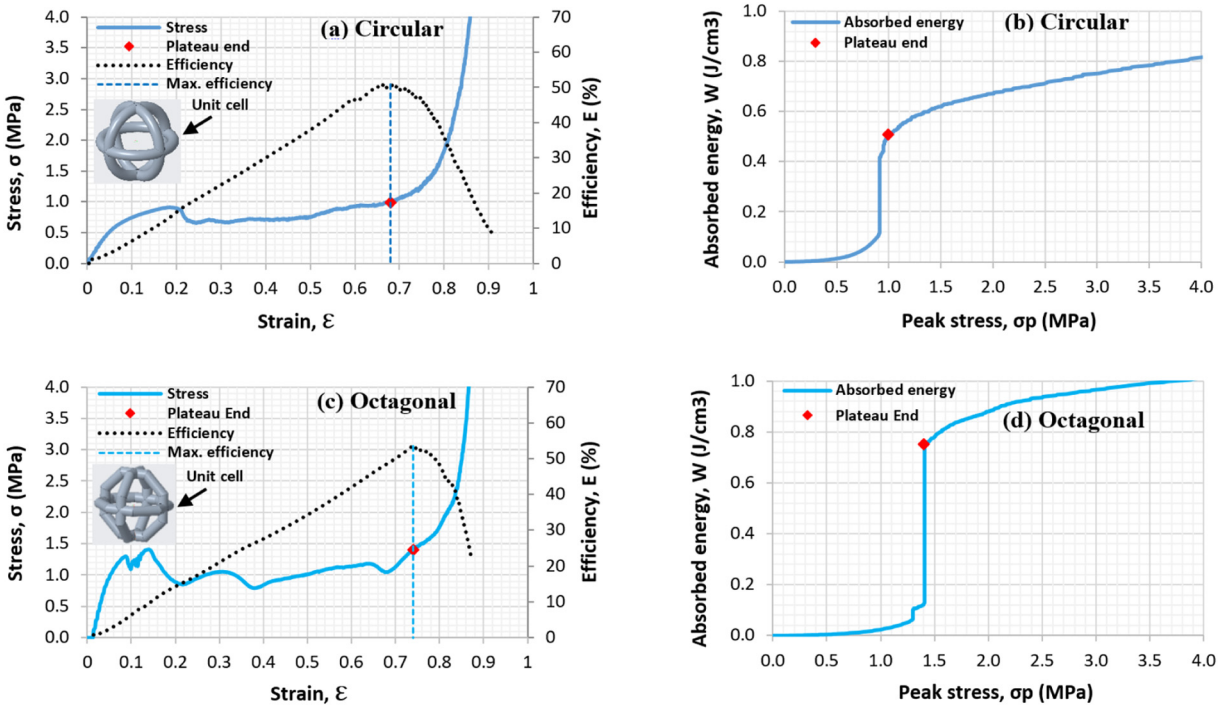

Fig. 6. Stress versus strain and energy absorption efficiency versus strain for (a) Circular and (c) Octagonal lattices, and their corresponding energy absorption diagrams for (b) Circular and (d) Octagonal lattices with plateau end indicated on the diagrams, all based on FEA.

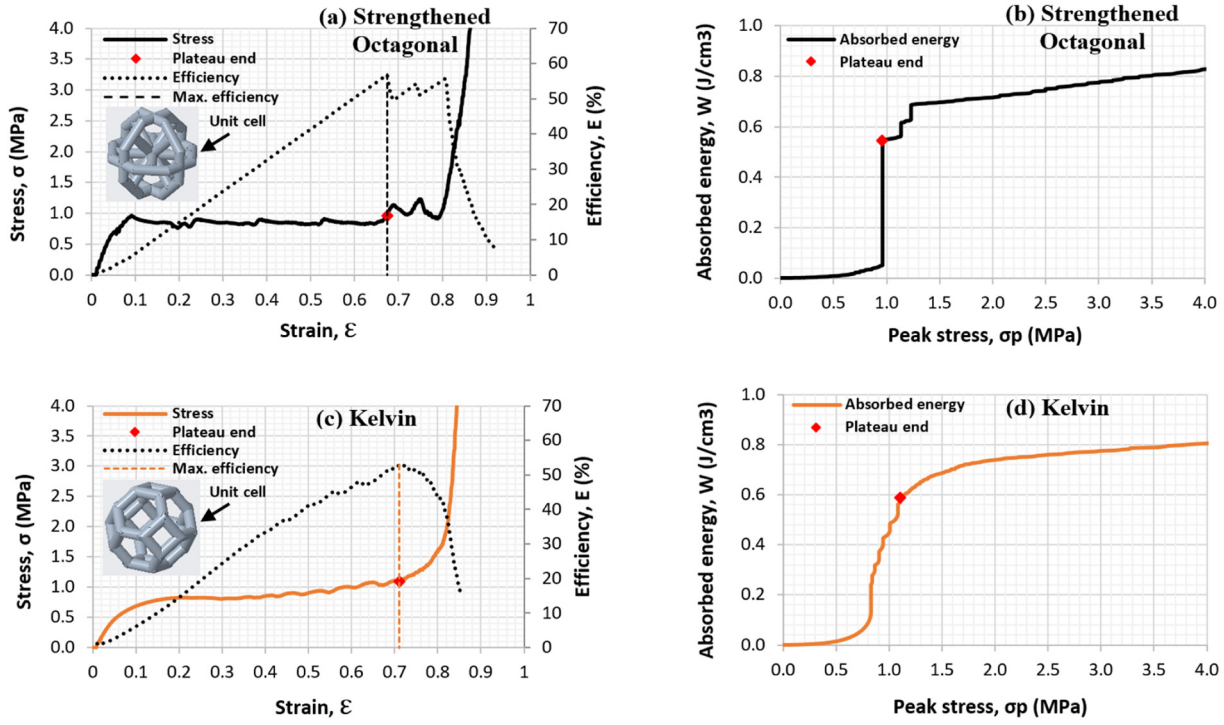

Fig. 7. Stress versus strain and energy absorption efficiency versus strain for (a) Strengthened Octagonal and (c) Kelvin lattices, and their corresponding energy absorption diagrams for (b) Strengthened Octagonal and (d) Kelvin lattices with plateau end indicated on the diagrams, all based on FEA.

rigid plates at the top and bottom of the lattice structures. All degrees of freedom of the bottom plate were set to zero. The top plate was allowed to move just in the vertical direction and compressed the lattices when moving downwards at a constant speed towards the bottom plate, as illustrated in Fig. 4a and b. In order to prevent the penetration of contacting surfaces during the crushing, a general contact algorithm (Explicit) was defined for the interaction of the lattice struts with themselves and with the top and bottom plates.

The compression simulation of each structure was performed up to the densification. The force and displacement data were obtained for

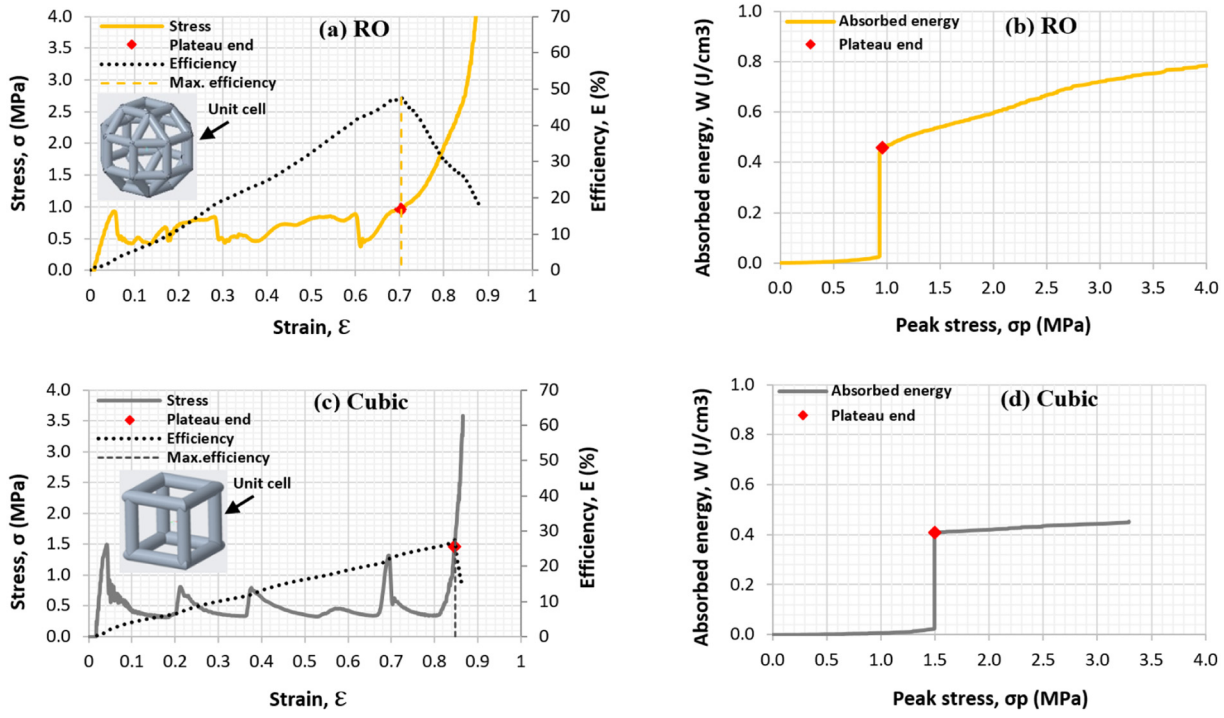

Fig. 8. Stress versus strain and energy absorption efficiency versus strain for (a) RO and (c) Cubic lattices, and their corresponding energy absorption diagrams for (b) RO and (d) Cubic lattices with plateau end indicated on the diagrams, all based on FEA.

Table 3
Energy absorption and compressive properties of the six HP PA12 lattices derived from the FEA stress-strain diagrams.

Type	Lattice designation	Plateau stress, σ_{pl} (MPa)	At the plateau end			
			Strain, ε_{cd}	Stress, σ (MPa)	Energy absorbed, W (J/cm^3)	Efficiency, E (%)
1	Circular	0.79	0.68	0.99	0.51	51
2	Octagonal	1.05	0.74	1.40	0.75	54
3	Strengthened Octagonal	0.85	0.67	0.96	0.55	57
4	Kelvin	0.89	0.71	1.10	0.59	53
5	RO	0.67	0.70	0.96	0.46	47
6	Cubic	0.48	0.85	1.46	0.41	27

1000 evenly spaced time intervals during the loading cycle as suggested by ISO 13314:2011 [40].

3.3. Numerical stress-strain diagrams

The compressive behaviour of cellular structures is commonly presented as the compressive stress-strain diagram, in which values of compressive stress, σ, are plotted as ordinates against corresponding values of compressive strain, ε, as abscissas [41]. Here, the compressive stress, σ, is the global stress and defined as the compressive load carried by the cellular solid specimen at any given moment divided by the original cross-sectional area of the specimen perpendicular to the loading direction expressed in force per unit area. The compressive strain, ε, is defined as the dimensionless ratio of reduction in the gage length at any given moment to the gage length of the cellular solid specimen along the loading direction.

Fig. 5 shows the schematic stress-strain behaviour of a typical cellular material under compressive loading. When an open cellular solid or foam is compressed, initially the cell edges bend giving a linear elastic deformation. At a certain stress level, the cell edges begin collapsing by elastic buckling, plastic yielding or brittle fracture, depending upon the cell material properties. Subsequent collapsing of the cells continues at an approximately constant stress, termed plateau stress. When all cell edges collapse and contact each other, the densification regime begins, and the stress increases rapidly. At the end of this final stage, the densified cellular solid behaves more like the dense parent material [3].

The compressive stress-strain diagrams of the investigated six lattice structures in this work under quasi-static displacement-controlled loading, as obtained from the FEA method described in Section 3.2 are presented in Figs. 6–8. The aforementioned three main regimes of the compressive behaviour of such structures, namely elastic, plateau and densification regimes, are apparent for each structure. Figs. 6–8 also show the efficiency versus strain and absorbed energy versus peak stress (energy absorption diagram) for all six structures that will be discussed in detail in later sections.

4. Energy absorption characterization of cellular structures

4.1. Densification strain

Plateau stress and densification strain are the most relevant properties of a cellular structure to its energy absorption characteristic [34]. The plateau of the stress-strain curve of a cellular structure ideally terminates at the densification strain, ε_d. Theoretically, ε_d is equal to the porosity $(1 - \rho^*/\rho_s)$ as it is the limiting strain at which all the pore space has been squeezed out. However, in reality, the cell edges jam together at a smaller strain than this [1].

The optimum use of such structures is up to the plateau end (also referred to as onset of densification), after which the stress increases significantly and become almost vertical at the densification strain [1], without much increase in energy absorption.

The plateau end (onset of densification) strain and the densification strain relate to different stages of interaction between cell edges, and hence to different points on the compressive stress-strain curve (refer to Fig. 5). However many publications do not distinguish between these two critical strains [42]. It was shown that the method based on the energy absorption efficiency diagram (as discussed in Section 4.5) gives unique, precise and consistent results to determine the plateau end strain, ε_{cd} [42]. According to this method, the plateau end strain of each stress-strain curve was calculated as the strain that provides the highest energy absorption efficiency. Figs. 6–8 illustrate the plateau end of each stress-strain curve determined by this method and the plateau end strain, ε_{cd}, for all lattices is listed in Table 3. Some other parameters are listed in the table, which will be discussed in detail in the next sections.

4.2. Plateau stress

From Fig. 5 it can be observed that the amount of energy absorbed in the initial elastic regime is very small and most of the energy is absorbed in the plateau regime nearly at a constant stress level. Hence, the energy absorption capability and characteristic of any cellular structure mainly depend on the plateau stress magnitude and the plateau length. For a given relative density, the higher, the more stable (nearly constant) and the longer the stress plateau is, the better is the energy absorption performance.

For a typical cellular solid, as shown in Fig. 5, the plateau regime starts from the crush (yield) strain, ε_y, representing the initiation of a new deformation mechanism of the cell edges, and ends at a critical strain, ε_{cd}, representing the end of stress plateau or onset of densification. The plateau stress is given by the equation [42],

$$\sigma_{pl} = \frac{\int_{\varepsilon_y}^{\varepsilon_{cd}} \sigma(\varepsilon)d\varepsilon}{\varepsilon_{cd} - \varepsilon_y} \tag{3}$$

or simply it is the average of stress in the plateau region. For the studied lattice structures, the crush strain ε_y was determined as the first point

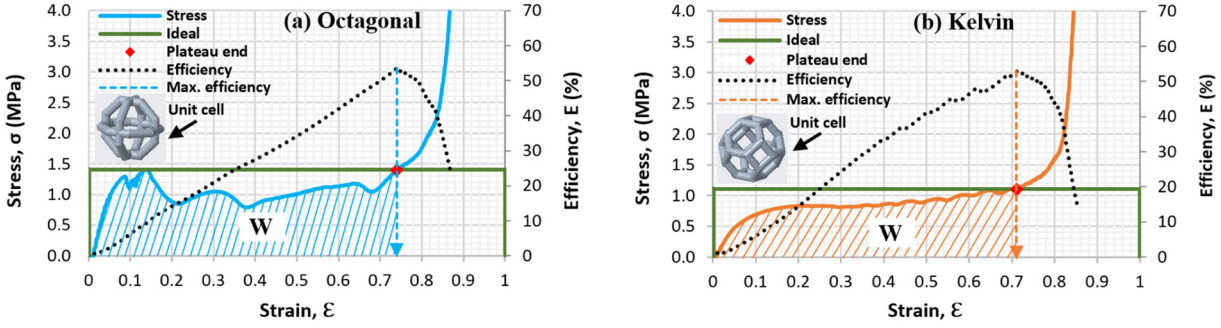

Fig. 9. Comparison of FEA efficiency parameter at the plateau end between the MJF HP PA12 (a) Octagonal and (b) Kelvin lattices.

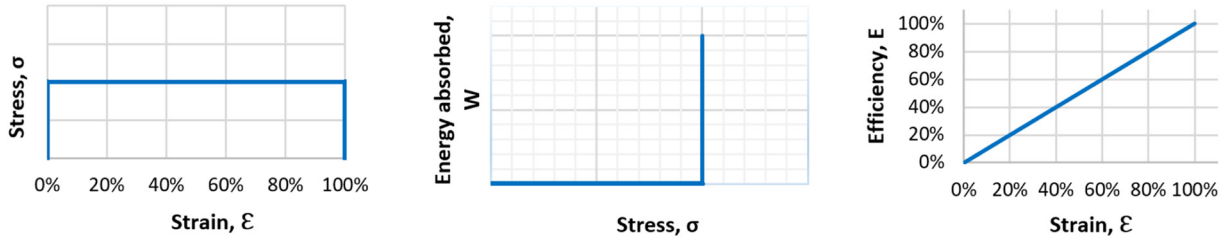

Fig. 10. Schematic (a) stress-strain, (b) energy absorption (energy absorbed vs peak stress) and (c) efficiency vs strain diagrams of an ideal energy absorber.

on the stress-strain diagram at which an increase in strain occurs without an increase in stress if that occurred before the strain of 0.1. Otherwise, as in Circular and Kelvin lattices, the ε_y was taken as the strain of 0.1 [41]. And, the efficiency diagram (Section 4.5) was used to determine the plateau end strain, ε_{cd}. The calculated plateau stress for all studied lattice structures is listed in Table 3. Among all structures, the Octagonal lattice provides the highest plateau stress of 1.05 MPa.

4.3. Energy absorption

The energy absorbed per unit volume, W, by a cellular structure under compressive loading up to a strain ε is represented by the area under the compressive stress-strain curve up to the strain ε and given by [43].

$$W = \int_0^{\varepsilon} \sigma(\varepsilon) d\varepsilon \tag{4}$$

The cumulative area under each curve up to each 1000 strain intervals was calculated in Microsoft Excel using a numerical method, namely trapezoidal rule [44]. The energy absorption of each lattice at the end of plateau region, which is the optimum use of each structure [1] is listed in Table 3. From the table, it can be seen that the Octagonal lattice is capable of absorbing the highest energy of 0.75 J/cm^3.

4.4. Energy absorption diagram

The energy absorption diagram [45] is a widely used engineering design tool for characterizing the energy absorption behaviour of materials and structures. It presents the relation between the two most important parameters for protective devices and packaging materials. It describes the amount of energy absorbed per unit volume, W, by a cellular material up to a strain ε as a function of the corresponding peak produced stress, σ_p, on the protected object. From the diagram, it can be determined whether an energy absorber is capable of absorbing a particular amount of energy within the limited stress threshold to keep the protected object safe.

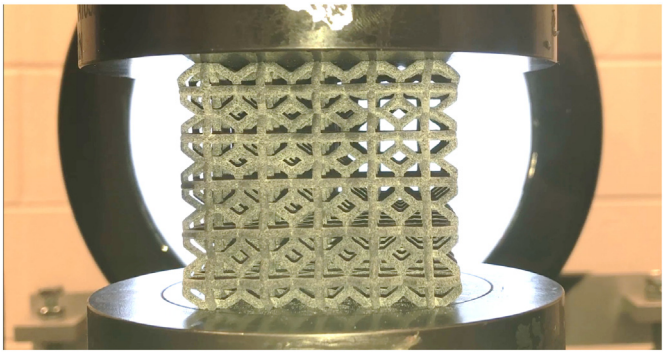

Fig. 11. Mechanical compression test setup.

The energy absorption diagram for the studied lattice structures is obtained by plotting the energy absorbed, W, against the peak produced stress, σ_p, up to each of 1000 strain intervals. The energy absorption diagrams of the studied lattice structures are shown in Figs. 6–8. It can be observed that the plateau end, which was calculated as the point that provides the highest energy absorption efficiency, represents the shoulder point on the energy absorption diagram precisely, which is consistent with the Maiti et al. [45] and Gibson and Ashby's [1] explanation.

4.5. Energy absorption efficiency

The efficiency parameter is the ratio of the energy absorbed by a material or structure up to a strain ε to the energy absorbed by an ideal energy absorber when both produce the same peak stress [46].

The efficiency parameter at the plateau end for the Octagonal and Kelvin lattices is illustrated in Fig. 9. It is equal to the area under each curve, W, up to the plateau end divided by the area under their corresponding ideal energy absorber (the green rectangular) which has a height of magnitude equal to the stress at the plateau end and a length of 1 (100% strain).

The efficiency parameter, E, at a strain, ε is given by [46]:

$$E = \frac{\int_0^{\varepsilon} \sigma(\varepsilon) d\varepsilon}{\sigma_p * 1} \tag{5}$$

where σ_p is the peak produced stress up to a given strain, ε.

In other words, the efficiency parameter, E, at any strain, ε, is simply equal to the ratio of the energy absorbed to the peak produced stress σ_p up to the strain ε.

Herein the ideal energy absorber needs to be defined. Such a structure or material is the one which provides a rectangular stress-strain curve under compressive loading [34] as shown in Fig. 10a. An ideal structure does not deform initially (shows a rigid behaviour with no initial elastic region) until the stress reaches the compressive strength of the energy absorber where the cells begin collapsing at a constant stress (plateau stress) up to 100% strain. It has the longest possible stress plateau, from the strain interval 0 to 1 without densification. In reality, there are foams made with a relative density as small as 0.001 [1], which theoretically means it can undergo up to 99.9% strain. The energy absorption diagram of an ideal energy absorber is shown in Fig. 10b.

The schematic energy absorption diagram of an ideal energy absorber is shown in Fig. 10b. It can be seen that there is no energy absorption up to a certain stress (plateau stress), then the energy absorption goes up vertically at that constant stress. The efficiency of an ideal energy absorber (Fig. 10c) has a linear relationship with strain. It starts from 0% at 0 strain and reaches 100% at 100% strain.

The efficiency-strain diagrams for the lattice structures are shown on the stress-strain diagrams in Figs. 6–8 and the plateau end strain was determined as the strain which provides the highest energy absorption efficiency as suggested by Li [42]. Among the six lattices, the Strengthened Octagonal and Octagonal lattices provide the highest energy absorption efficiency of 57% and 54% as listed in Table 3.

Some researchers have investigated the energy absorption capability of such materials using the so-called ideality parameter [26,43,46],

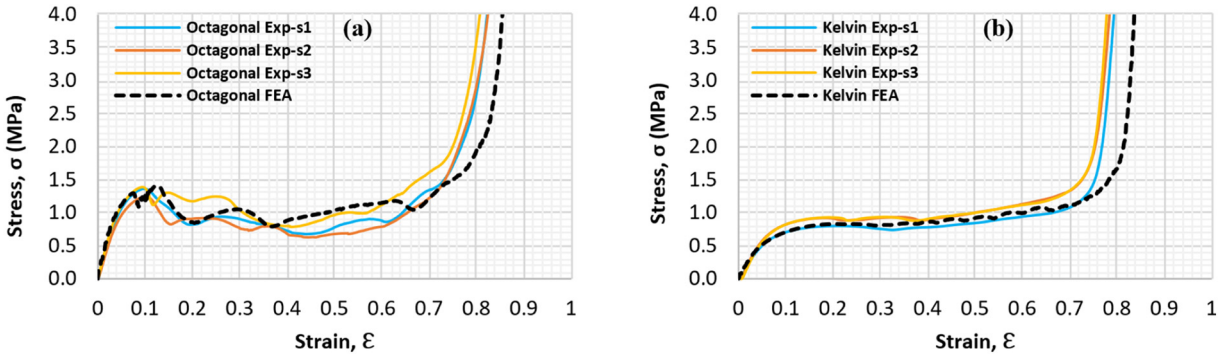

Fig. 12. Comparing the simulation (FEA) with the experimental (Exp) compressive stress-strain curves of HP PA12 lattices of (a) Octagonal and (b) Kelvin unit cells.

which is the ratio between the energy absorbed by a cellular solid to the energy absorbed by an ideal energy absorber when both are compressed to the same strain, and produce the same peak stress [46]. However, it was found that the ideality parameter cannot provide satisfactory results regarding the capability of cellular structures for absorbing energy [43].

5. Experimental validation

5.1. Compression tests of lattices

To further investigate the compression response of lattice structures experimentally and validate the FEA compression results, two types of lattices (Octagonal and Kelvin) with the highest energy absorption predicted by FEA method (Table 3) were selected for compression tests. Three specimens of each of these two lattices were tested under quasi-static uniaxial displacement-controlled loading. The same aforementioned universal testing machine (MTS Criterion Model 43) was used for the compression tests. The tests were performed at room temperature by placing a specimen on the lower fixed platform. The crosshead was moving downwards at a constant speed of 5 mm/min in accordance with the standard test method for compressive properties of rigid cellular plastics ASTM 1621-16 [47]. Fig. 11 shows the compression test setup of an Octagonal lattice sample. The force-displacement data is recorded during the test on a connected computer. This data was converted to stress-strain data in the same way as explained in Section 3.3. The experimental stress-strain curves of three samples of both Octagonal and Kelvin lattices are compared to their FEA results in Fig. 12.

It can be noticed from Fig. 12 that the FEA approach used is in good agreement with the experimental results. However, as reported in the previous studies [37,48] the FEA approach predicts a higher densification strain, much closer to the theoretical prediction [37] than the experimental results, which causes some variance in the FEA and experimental results. The experimental energy absorption efficiency for the Octagonal lattice is found to be 48% versus 54% predicted by the FEA method, and for the Kelvin lattice, they were 49% vs 53% respectively.

5.2. MJF process vs. FDM

A prototype of each lattice also made by fused deposition modeling (FDM) process. Fortus 450mc FDM by Stratasys, which is one of the most powerful FDM systems currently available on the market, was used for printing the lattices. Careful attention was paid to choose appropriate process parameters to make sure the lattices would be printed properly. The lattices are constructed from cylindrical struts of small diameters ranging from 1.134 to 2.246 mm (refer to Table 1). To be able to print the cross-section of these cylindrical struts appropriately the smallest tip size (T12) available for Nylon12 (with the layer thickness of 0.1778 mm), and the smallest raster width of 0.254 mm were used. An Octagonal lattice sample made by this process (FDM) is compared to the same lattice made by MJF process in Fig. 13 and optical micrographs of a sample of each 3D printing process are shown in Fig. 14. It can be observed that the MJF part's appearance and quality are much better compared to the FDM sample. The time needed to print 4 lattices on FDM was 93 h and 16 min while for 12 lattices it took 3 h and 39 min. Which means the MJF required 0.013 fraction of the time required for the FDM process. The quasi-static compressive stress-strain curves of

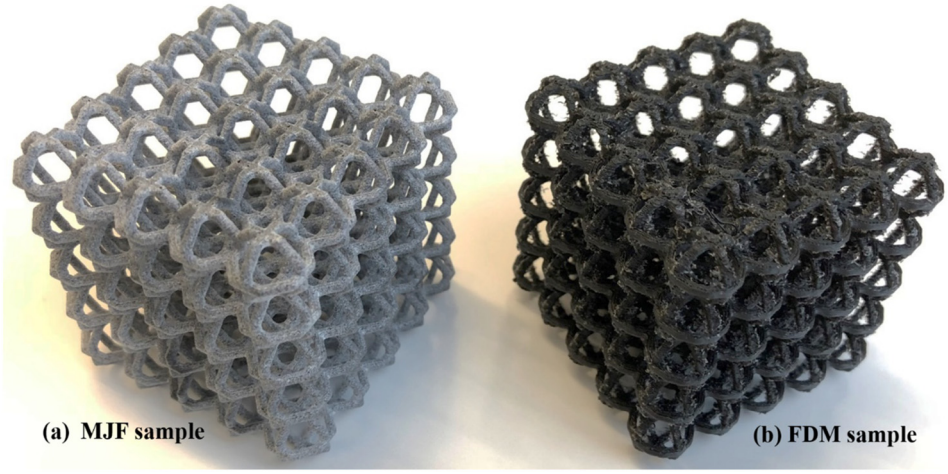

Fig. 13. An Octagonal lattice sample built by HP Jet Fusion 4200 (MJF) compared to a sample built by Fortus 450mc (FDM).

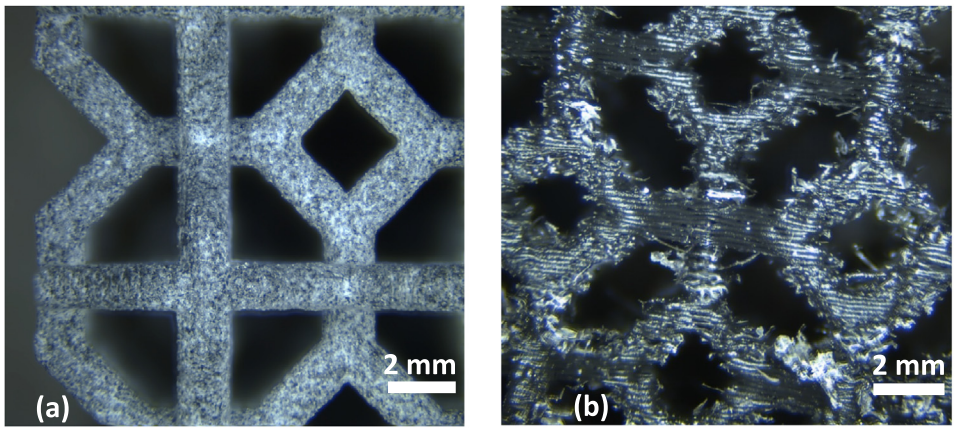

Fig. 14. Optical micrographs of (a) MJF sample and (b) FDM sample.

MJF vs. FDM Octagonal lattice samples are compared in Fig. 15. It can be seen that the MJF sample provides much higher modulus, crush strength and energy absorption than the FDM sample. It was also observed that the FDM samples tear apart after the compression tests whereas the MJF samples showed no signs of rupture in the lattices struts after being fully compressed, and they even had good recovery behaviour, as shown in Fig. 16.

6. Discussion of results

From the comparison of MJF with the FDM lattices and their compression behaviour it was observed that the newly developed MJF process, could produce the lattice structures with much higher quality and functionality in 0.013 fraction of time needed for FDM process.

The analysis of the FEA data, compression response and energy absorption behaviour of the lattices showed that the lattices which deform by bending under the compression loading such as Circular, Octagonal, Strengthened Octagonal and Kelvin lattices generally provide good energy absorption characteristic (high energy absorption and efficiency). Among the six studied structures, the Octagonal lattice is identified as the optimum structure with the closest performance to the ideal energy absorber. It provides the highest plateau stress of 1.05 MPa, the highest energy absorption per unit volume of 0.75 J/cm^3, and the second highest efficiency of 54% as listed in Table 3. The high energy absorption performance of the 3D Octagonal lattice was found to be consistent with the results of 2D Octagonal honeycomb reported in [26]. The compressive response of the RO type lattice is stretching dominated and the Cubic lattice is buckling dominated, which makes them stiff and strong but unsuitable for energy absorption due to the significant softening of these structures after the yield point. These two lattices have the minimum energy absorption of 0.46 J/cm^3 and 0.41 J/cm^3 and minimum efficiency of 47% and 27% respectively.

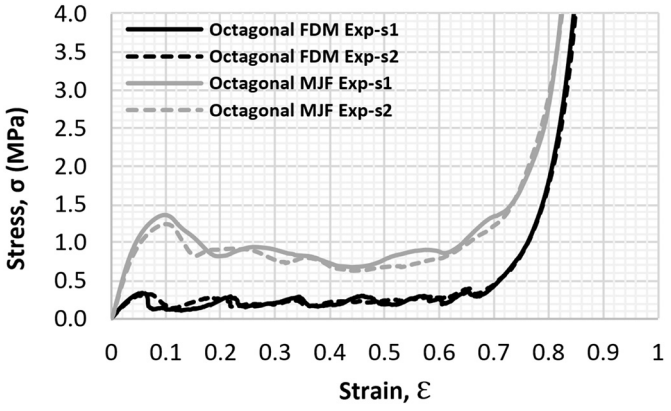

Fig. 15. Quasi-static experimental (Exp) compressive stress-strain curves of MJF vs FDM Octagonal lattice samples.

It was observed that when keeping the relative density constant, adding extra inclined struts to strengthen the Octagonal lattice of type 2, caused an increase in efficiency from 54% to 57%. This is due to the more stable stress plateau of the Strengthened Octagonal compared to the Octagonal lattice. However, the energy absorption dropped significantly from 0.75 to 0.55 J/cm^3, caused by a shorter plateau.

The nonlinear FEA method used in this study provided predictions which were in good agreement with the experimental test results obtained from two types of lattices built by MJF. However, the FEA results predicted a slightly higher densification strain, and thus longer stress plateau, which resulted in overestimating energy absorption and efficiency. The methodology adopted in this study to determine the plateau end (onset of densification) by using the efficiency method, was precisely consistent with the shoulder point on the energy absorption diagram as reported by Maiti et al. [45] and Gibson and Ashby [1]. The Octagonal and Kelvin lattices investigated experimentally in this study were found to provide higher energy absorption efficiency, 48% and 49% respectively, when compared to the Octet-truss and all other cellular materials reported in [25] including the Aluminum foam and honeycomb.

7. Conclusions

This investigation aimed to develop a high energy-absorbing lattice with the closest behaviour to the ideal energy absorber. The compressive stress-strain response and energy absorption characteristics of lattice structures from six different types of unit cells with identical relative density were evaluated and compared. A recently developed 3D printing process, namely Multi Jet Fusion (MJF), was successfully used to print high-quality prototypes of the lattices in a brand of polyamide (nylon) 12. Full-scale nonlinear FEA was used to investigate the compressive behaviour of lattices. The mechanical tests performed on two types of the lattices, Octagonal and Kelvin lattices, were in good agreement with the FEA predictions. Clear trends were observed on the influence of unit cell configuration on plateau stress, energy absorption and efficiency. In terms of plateau stress, the lattices with bending-dominated deformation were found to be compliant and display a relatively stable plateau region resulting in higher energy absorption and efficiency. On the other hand, those with stretching and buckling dominated deformation were found to be much stiffer and stronger, but soften after yielding, thus causing a lower energy absorption and efficiency.

The results have identified that under quasi-static loading the Octagonal lattice offers the optimum energy absorption characteristic among the six types of studied unit cell structures. It provides a high plateau stress, energy absorption and efficiency of 1.05 MPa, 0.75 J/cm^3 and

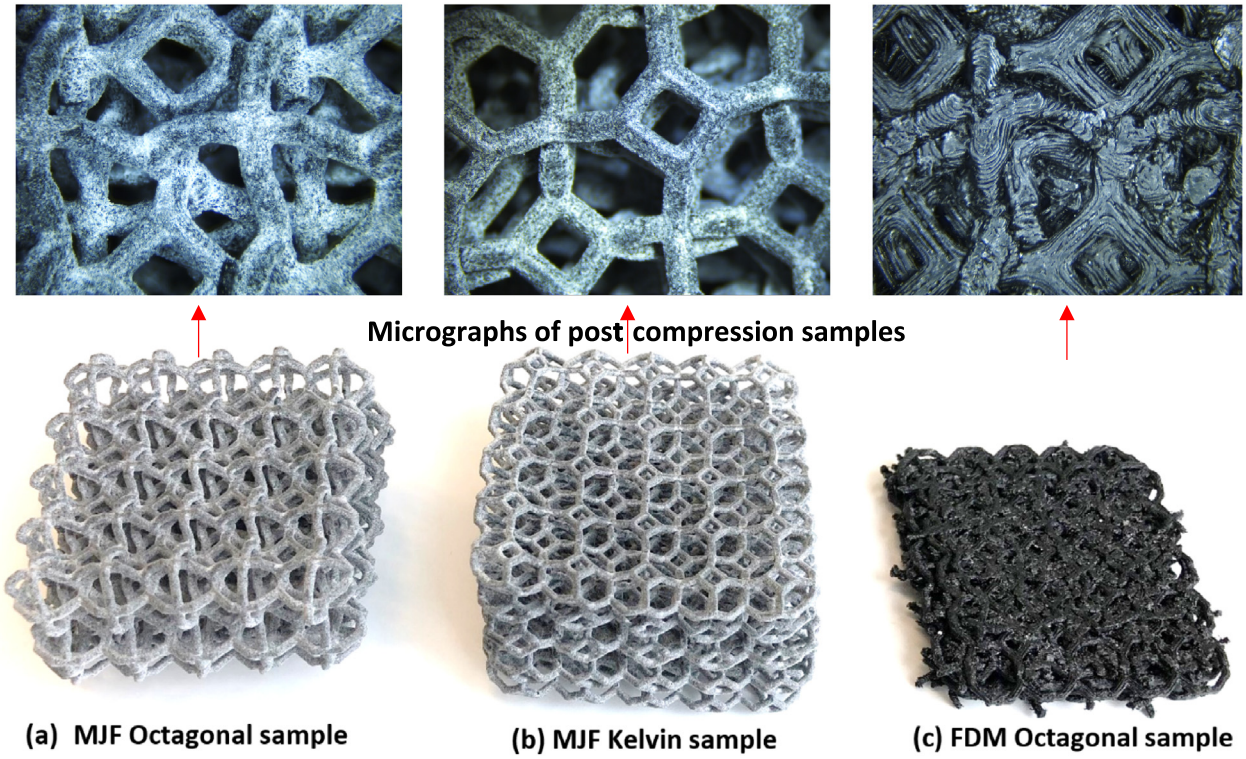

Fig. 16. Post-compression test samples built by MJF compared to an FDM sample.

54% respectively. The results of this study reveal a strong relationship between the morphological and energy absorption properties of the lattice structures. The findings give a greater understanding on designing and 3D printing of lattice structures with the closest behaviour to the ideal energy absorber and can help to develop advanced lattice materials that are superior to the currently used stochastic foams. This study focussed only on using the quasi-static displacement loading to examine the energy absorption behaviour of the studied structures. However, in impact applications, these structures will be exposed to various dynamic loading conditions depending on the application, which may cause a difference in their energy absorption behaviour. Hence, further studies are needed to investigate their performance under specified dynamic loading conditions.

References

[1] L.J. Gibson, M.F. Ashby, Cellular Solids: Structure and Properties, second edition Cambridge University Press, Cambridge, 1997 1–510.
[2] E.B. Duoss, T.H. Weisgraber, K. Hearon, C. Zhu, W. Small, T.R. Metz, J.J. Vericella, H.D. Barth, J.D. Kuntz, R.S. Maxwell, C.M. Spadaccini, T.S. Wilson, Three-dimensional printing of elastomeric, cellular architectures with negative stiffness, Adv. Funct. Mater. 24 (31) (2014) 4905–4913.
[3] M.F. Ashby, The properties of foams and lattices, Philos. Trans. R. Soc. A-Math. Phys. Eng. Sci. 364 (1838) (2006) 15–30.
[4] V. Srivastava, R. Srivastava, On the polymeric foams: modeling and properties, J. Mater. Sci. 49 (7) (2014) 2681–2692.
[5] Z. Ozdemir, E. Hernandez-Nava, A. Tyas, J.A. Warren, S.D. Fay, R. Goodall, I. Todd, H. Askes, Energy absorption in lattice structures in dynamics: experiments, Int. J. Impact Eng. 89 (2016) 49–61.
[6] F.N. Habib, M. Nikzad, S.H. Masood, A.B.M. Saifullah, Design and development of scaffolds for tissue engineering using three-dimensional printing for bio-based applications, 3D Print. Addit. Manuf. 3 (2) (2016) 119–127.
[7] A. Kantaros, N. Chatzidai, D. Karalekas, 3D printing-assisted design of scaffold structures, Int. J. Adv. Manuf. Technol. 82 (1–4) (2016) 559–571.
[8] P. Pooyan, R. Tannenbaum, H. Garmestani, Mechanical behavior of a cellulose-reinforced scaffold in vascular tissue engineering, J. Mech. Behav. Biomed. Mater. 7 (2012) 50–59.
[9] T. Serra, M. Ortiz-Hernandez, E. Engel, J.A. Planell, M. Navarro, Relevance of PEG in PLA-based blends for tissue engineering 3D-printed scaffolds, Mater. Sci. Eng. C 38 (2014) 55–62.
[10] I. Zein, D.W. Hutmacher, K.C. Tan, S.H. Teoh, Fused deposition modeling of novel scaffold architectures for tissue engineering applications, Biomaterials 23 (4) (2002) 1169–1185.
[11] E. Linul, D.A. Serban, T. Voiconi, L. Marsavina, T. Sadowski, Energy - absorption and efficiency diagrams of rigid PUR foams, in: L. Marsavina (Ed.), Proceedings of the 14th Symposium on Experimental Stress Analysis and Materials Testing 2014, pp. 246–249.
[12] S.M. Ahmadi, S.A. Yavari, R. Wauthle, B. Pouran, J. Schrooten, H. Weinans, A.A. Zadpoor, Additively manufactured open-cell porous biomaterials made from six different space-filling unit cells: the mechanical and morphological properties, Materials 8 (4) (2015) 1871–1896.
[13] J. Brennan-Craddock, D. Brackett, R. Wildman, R. Hague, The Design of Impact Absorbing Structures for Additive Manufacture, Journal of Physics: Conference SeriesIOP Publishing, 2012.
[14] M. Vesenjak, L. Krstulovic-Opara, Z. Ren, Z. Domazet, Cell shape effect evaluation of polyamide cellular structures, Polym. Test. 29 (8) (2010) 991–994.
[15] C.I. Hammetter, R.G. Rinaldi, F.W. Zok, Pyramidal lattice structures for high strength and energy absorption, J. Appl. Mech. 80 (4) (2013), 041015. .
[16] Z. Ozdemir, A. Tyas, R. Goodall, H. Askes, Energy absorption in lattice structures in dynamics: nonlinear FE simulations, Int. J. Impact Eng. 102 (2017) 1–15.
[17] I. Ullah, M. Brandt, S. Feih, Failure and energy absorption characteristics of advanced 3D truss core structures, Mater. Des. 92 (2016) 937–948.
[18] R. Gautam, S. Idapalapati, S. Feih, Printing and characterisation of Kagome lattice structures by fused deposition modelling, Mater. Des. 137 (2018) 266–275.
[19] C.S. Ha, R.S. Lakes, M.E. Plesha, Design, fabrication, and analysis of lattice exhibiting energy absorption via snap-through behavior, Mater. Des. 141 (2018) 426–437.
[20] M. Kaur, T.G. Yun, S.M. Han, E.L. Thomas, W.S. Kim, 3D printed stretching-dominated micro-trusses, Mater. Des. 134 (2017) 272–280.
[21] S.Y. Choy, C.-N. Sun, K.F. Leong, J. Wei, Compressive properties of functionally graded lattice structures manufactured by selective laser melting, Mater. Des. 131 (2017) 112–120.
[22] D.S. Al-Saedi, S. Masood, M. Faizan-Ur-Rab, A. Alomarah, P. Ponnusamy, Mechanical properties and energy absorption capability of functionally graded F2BCC lattice fabricated by SLM, Mater. Des. 144 (2018) 32–44.
[23] J. Harris, R. Winter, G.J. Mcshane, Impact response of additively manufactured metallic hybrid lattice materials, Int. J. Impact Eng. 104 (2017) 177–191.
[24] R. Winter, M. Cotton, E. Harris, D. Eakins, G. McShane, High resolution simulations of energy absorption in dynamically loaded cellular structures, Shock Waves 27 (2) (2017) 221–236.
[25] M. Mohsenizadeh, F. Gasbarri, M. Munther, A. Beheshti, K. Davami, Additively-manufactured lightweight Metamaterials for energy absorption, Mater. Des. 139 (2018) 521–530.
[26] F.N. Habib, P. Iovenitti, S.H. Masood, M. Nikzad, Cell geometry effect on in-plane energy absorption of periodic honeycomb structures, Int. J. Adv. Manuf. Technol. 94 (5–8) (2018) 2369–2380.

[27] A. Fereidoon, S.A. Taheri, Using finite element method to analyze the effect of microstructure on energy absorption properties of open cell polymeric foams, J. Cell. Plast. 48 (3) (2012) 257–270.
[28] R.M. Sullivan, L.J. Ghosn, B.A. Lerch, A general tetrakaidecahedron model for open-celled foams, Int. J. Solids Struct. 45 (6) (2008) 1754–1765.
[29] G. Maîtrejean, P. Terriault, D. Devís Capilla, V. Brailovski, Unit cell analysis of the superelastic behavior of open-cell tetrakaidecahedral shape memory alloy foam under quasi-static loading, Smart Mater. Res. 2014 (2014).
[30] N. Chantarapanich, P. Puttawibul, S. Sucharitpwatskul, P. Jeamwatthanachai, S. Inglam, K. Sitthiseripratip, Scaffold library for tissue engineering: a geometric evaluation, Comput. Math. Methods Med. 2012 (2012).
[31] A. Boccaccio, M. Fiorentino, A.E. Uva, L.N. Laghetti, G. Monno, Rhombicuboctahedron unit cell based scaffolds for bone regeneration: geometry optimization with a mechanobiology–driven algorithm, Mater. Sci. Eng. C 83 (2018) 51–66.
[32] HP Jet Fusion 3D printing. [13/03/2018], Available from www.hp.com/go/3DPrint.
[33] A. Standard, D638-14 Standard Test Method for Tensile Properties of Plastics, ASTM International, West Conshohocken, PA, 2014.
[34] G. Lu, T. Yu, in: T.X. Yu (Ed.), Energy absorption of structures and materials, Woodhead, Cambridge, 2003.
[35] W.D. Callister, D.G. Rethwisch, Materials Science and Engineering, 8th ed.vol. 5, John Wiley & Sons NY, USA/Versailles, 2011.
[36] SYSTEMES, D., Simulia, Abaqus 6.12 Analysis User's Manual, Volume III: Materials, 2012.
[37] F.N. Habib, P. Iovenitti, S.H. Masood, M. Nikzad, In-plane energy absorption evaluation of 3D printed polymeric honeycombs, Virtual Phys. Prototyp. 12 (2) (2017) 117–131.
[38] SYSTEMES, D., Simulia, ABAQUS/CAE User's Manual. ABAQUS Documentation V6, 2014 7.
[39] H. Altenbach, A. Öchsner, Cellular and Porous Materials in Structures and Processes, vol. 521, Springer Science & Business Media, 2011.
[40] I. Standard, ISO 13314: 2011 (E) Mechanical Testing of Metals—Ductility Testing—Compression Test for Porous and Cellular Metals. Ref Number ISO. 13314(13314), 2011 1–7.
[41] ASTM, D., 1621, Standard Test Method for Compressive Properties Of Rigid Cellular Plastics, American Society for Testing and Materials, New York, 2010.
[42] Q.M. Li, I. Magkiriadis, J.J. Harrigan, Compressive strain at the onset of densification of cellular solids, J. Cell. Plast. 42 (5) (2006) 371–392.
[43] M. Avalle, G. Belingardi, R. Montanini, Characterization of polymeric structural foams under compressive impact loading by means of energy-absorption diagram, Int. J. Impact Eng. 25 (5) (2001) 455–472.
[44] S.C. Chapra, R.P. Canale, Numerical Methods for Engineers, vol. 2, McGraw-Hill, New York, 2015.
[45] S. Maiti, L. Gibson, M. Ashby, Deformation and energy absorption diagrams for cellular solids, Acta Metall. 32 (11) (1984) 1963–1975.
[46] J. Miltz, O. Ramon, Energy absorption characteristics of polymeric foams used as cushioning materials, Polym. Eng. Sci. 30 (2) (1990) 129–133.
[47] A.I. Publisher, Standard Test Method for Compressive Properites of Rigid Celluar Plastics: ASTM D1621-16, SAI Global, Perth, W.A., 2012
[48] S.D. Papka, S. Kyriakides, In-plane crushing of a polycarbonate honeycomb, Int. J. Solids Struct. 35 (3) (1998) 239–267.